JACC: CARDIOVASCULAR IMAGING
VOL. ■, NO. ■, 2017

ISSN 1936-878X/$36.00
PUBLISHED BY ELSEVIER
http://dx.doi.org/10.1016/j.jcmg.2016.12.019

3D Morphological Changes in LV and RV During LVAD Ramp Studies

Karima Addetia, MD,[a] Nir Uriel, MD,[a] Francesco Maffessanti, PhD,[a] Gabriel Sayer, MD,[a] Sirtaz Adatya, MD,[a] Gene H. Kim, MD,[a] Nitasha Sarswat, MD,[a] Savitri Fedson, MD,[a] Diego Medvedofsky, MD,[a] Eric Kruse, RDCS,[a] Keith Collins, MS,[a] Daniel Rodgers, PhD,[a] Takayoshi Ota, MD, PhD,[a] Valluvan Jeevanandam, MD,[a] Victor Mor-Avi, PhD,[a] Daniel Burkhoff, MD, PhD,[b,c] Roberto M. Lang, MD[a]

ABSTRACT

OBJECTIVES The purpose of this study was to investigate the differential impact of the 2 most commonly available left ventricular assist device (LVAD) types on the right (RV) and left (LV) ventricles using 3-dimensional (3D) echocardiography-based analysis of ventricular morphology.

BACKGROUND LVADs have emerged as common therapy for advanced heart failure. Recent data suggest that the heart responds differently to speed settings in the 2 main devices available (HeartMate II [HMII], St Jude Medical, Pleasanton, California, and HVAD, HeartWare International, Framingham, Massachusetts). We hypothesized that 3D echocardiographic assessment of LV and RV volumes and shape would help describe the differential impact of the 2 LVAD types on the heart.

METHODS Simultaneous 3D echocardiography, ramp test, and right heart catheterization were performed in 31 patients with LVADs (19 with HMII and 12 with HVAD). Device speed was increased stepwise (8,000 to 12,000 for HMII and 2,300 to 3,200 revolutions per minute for HVAD). 3D echocardiographic full-volume LV and RV datasets were acquired, and endocardial surfaces were analyzed using custom software to calculate LV sphericity, conicity (perfect sphere/cone = 1) and RV septal and free-wall curvature (0 = flat; <0 = concave; >0 = convex).

RESULTS For both devices, cardiac output increased and wedge pressure decreased with increasing speed. In HMII, LV volumes progressively decreased (meanΔ = 127 ml) as the LV became less spherical and more conical, whereas the RV volume initially remained stable, but subsequently increased at higher speeds (meanΔ = 60 ml). Findings for the HVAD were similar, but less pronounced (LV:meanΔ = 51 ml, RV:meanΔ = 22 ml), and the LV remained significantly more spherical even at high speeds. On average, in HMII patients, the RV septum became more convex (bulging into the LV) at the highest speeds whereas in HVAD patients, there was no discernable change in the RV septum.

CONCLUSIONS The heart responds differently to pump speed changes with the 2 types of LVAD, as reflected by the volume and shape changes of both the LV and RV. Our study suggests that adding RV assessment to the clinical echo-ramp study may better optimize LVAD speed. Further study is needed to determine whether this would have an impact on patient outcomes. (J Am Coll Cardiol Img 2017;■:■–■) © 2017 by the American College of Cardiology Foundation.

Worldwide use of continuous-flow left ventricular assist devices (cfLVADs) is growing. Additionally, an increasing number of patients are being considered for destination therapy, and as a result, patients are being supported for increasingly longer periods of time (1,2). Accordingly, there is a growing need to find more optimal ways to manage these patients,

From the [a]Department of Medicine, Section of Cardiology, University of Chicago, Chicago, Illinois; [b]Columbia University Medical Center, New York, New York; and the [c]Cardiovascular Research Foundation, New York, New York. Dr. Uriel has received grant support from HeartWare and Thoratec; and has served as a consultant for Thoratec, HeartWare, Abiomed, and Medtronic. Dr. Jeevanandam has served as a consultant for Thoratec; and as a scientific advisor to Thoratec, Reliant Heart, and HeartWare. Dr. Burkhoff is a consultant to HeartWare division of Medtronic. Dr. Lang serves on the speakers and advisory bureaus of Philips

ABBREVIATIONS AND ACRONYMS

2D = 2-dimensional

3D = 3-dimensional

cfLVAD = continuous-flow left ventricular assist device

HMII = HeartMate II

LV = left ventricle/ventricular

RPM = revolutions per minute

RV = right ventricle/ventricular

TTE = transthoracic echocardiography

one important facet being proper setting of device speed. Current recommendations for device speed adjustments are based on hemodynamics and echocardiographic parameters measured during "ramp" studies, in which cfLVAD speed is gradually increased over a range tolerated by the patient (3). Optimal speed is opined to be the one at which aortic valve opening is intermittent, the interventricular septum is midline, and mitral and aortic regurgitation are minimized together with pulmonary capillary wedge pressure <18 mm Hg and central venous pressure <12 mm Hg (3). Accordingly, one cannot rule out that additional factors may prove helpful in device speed optimization, and identifying them may have an impact on optimal use of these devices and thus on patient outcomes.

Two-dimensional (2D) imaging studies have shown that hearts supported with different types of cfLVADs (centrifugal vs. axial) respond differently to changes in speed from an anatomic perspective (4-6), raising the question whether different criteria need to be established for speed optimization in these 2 cfLVAD types. Invasive measurements have shown that both types of devices perform similarly in response to speed changes in terms of flow, and central and peripheral pressures (6). This has led to the hypothesis that perhaps device location, that is, intrathoracic (HVAD, HeartWare International, Framingham, Massachusetts) versus extrathoracic (HeartMate II [HMII], St Jude Medical, Pleasanton, California) has an anatomic impact on the native heart. If so, device location not only may impact how the left ventricle responds to changes in speed, but may also impact, via different effects on the septum, right ventricular (RV) geometry, size, and function (7-9). We hypothesized that 3-dimensional (3D) echocardiography-derived parameters of size and shape of the 2 ventricles may provide additional information in this context. We therefore performed 3D echocardiographic imaging during hemodynamic ramp studies in patients supported with either a centrifugal cfLVAD (HVAD) or an axial cfLVAD (HMII) to determine how device speed influences global left ventricular (LV) and RV sizes and shapes, including an analysis of septal geometry. Our aims were: 1) to determine how device speed influences LV and RV size and shape, including septal geometry; and 2) to test the feasibility of 3D echocardiographic analysis during the cfLVAD ramp study.

METHODS

We prospectively considered 63 consecutive ramp studies performed in patients with either a centrifugal (HVAD) or an axial (HMII) cfLVAD who were referred for a clinically indicated ramp test with right heart catheterization for LVAD speed adjustment. Patients with poor 2D and/or 3D image quality or who did not meet ramp study safety criteria (see the following text) or who were undergoing a ramp test for reasons other than speed optimization were excluded from the analysis. Thirty-five patients were thereby selected. Of these 35, 4 did not complete the full ramp protocol. The final cohort consisted of 31 patients, including 19 with an HMII and 12 with an HVAD (**Table 1**). The study was approved by the institutional review board, and all patients provided informed consent.

All tests were performed in the catheterization laboratory. The overall methods employed in this study for hemodynamic assessment have been detailed previously (6). At the initiation of the study, pump speeds were lowered to 2,300 revolutions per minute (RPM) in patients with HVAD and 8,000 RPM in patients with HMII pumps. After a 5-min stabilization period, echocardiographic, hemodynamic, and device flow, power, and pulsatility index values were taken. After completion of data acquisition, device speeds were increased by 100-RPM increments for HVAD patients and by 400-RPM increments for HMII patients. After a 2-min stabilization period, hemodynamic parameters were recorded. 3D echocardiographic images were acquired at every other speed setting, that is, at 200-RPM increments for HVAD patients and at 800-RPM increments for HMII patients. This procedure was repeated until 1 of the following occurred: 1) a maximum speed of 3,200 RPM was reached for HVAD patients or 12,000 RPM for HMII patients; 2) a suction event; or 3) a decrease in LV end-diastolic diameter to <30 mm. To simplify the graphical presentation and pooling of data, ramp speed settings were labeled from Stage I (lowest speed) to Stage V (highest speed).

Medical Imaging; and has received research grants from Philips Medical Imaging. All other authors have reported that they have no relationships relevant to the contents of this paper to disclose. Drs. Uriel and Lang contributed equally to this work.

Manuscript received June 21, 2016; revised manuscript received October 12, 2016, accepted December 2, 2016.

3D TRANSTHORACIC ECHOCARDIOGRAPHY. 3D transthoracic echocardiography (TTE) full-volume datasets of the LV and RV using electrocardiogram gating over 4 to 6 consecutive cardiac cycles during a single breath-hold (10) were obtained (iE33 ultrasound, X5-1 transducer, Philips, Amsterdam, the Netherlands). Effort was made to maximize frame rate by imaging the RV and LV separately in order to decrease the sector width, and excluding the atria from the dataset to minimize depth. 3D TTE images of the LV were acquired from an LV-focused apical 4-chamber view, whereas a modified apical 4-chamber view focused on the RV was used for the RV.

3D TTE images were analyzed using commercial software (4D LV-Function and 4D RV-Function, version 2.0, TomTec Imaging Systems, Unterschleissheim, Germany) to quantify end-diastolic and end-systolic volumes and ejection fraction of both ventricles. End-diastole was identified automatically by the software as the time point at which the ventricular cavity was at its largest. Analysis required manual initialization of the contours in both end-systolic and end-diastolic frames in the apical 4-, 2-, and 3-chamber views in the case of the LV and in the long-axis and basal, mid, apical short-axis planes in the RV. 3D renderings of the LV and RV endocardial surface were then automatically generated and stored for input into custom software for shape analysis. All 3D data analysis and interpretation were performed independent of knowledge of the speed settings and hemodynamic results.

LV SHAPE ANALYSIS. The 3D LV endocardial surfaces were exported as a series of unstructured meshes of connected points that were used as input to a custom software package for analysis of LV conicity and sphericity via an algorithm described in detail previously and summarized in the upper portion of **Figure 1** (11,12). Briefly, LV global shape indices were defined by measuring the degree of similarity between the signal obtained by sampling along a helical pattern on the 3D LV surface and a signal obtained using the same procedure from an idealized, reference 3D shape, either a sphere or a cone (**Figure 1**, left side illustrates analysis for sphericity, right side illustrates analysis for conicity). In order to ensure the independence of LV shape indices from LV dimensions, the reference shapes were constructed for each individual heart according to geometric properties of each individual LV (principal moments of inertia). Accordingly, the indices of sphericity and conicity assume values between 0 and 1, with higher values associated with a better similarity to the relevant reference shape.

TABLE 1 Baseline Patient Characteristics

	All (N = 31)	HMII (n = 19)	HVAD (n = 12)	p Value*
Age, yrs	58 ± 11	60 ± 10	56 ± 13	0.29
Male	17	10	7	NS
BSA, m^2	2.0 ± 0.3	2.0 ± 0.3	1.8 ± 0.3	0.03
Implant to ramp, months	42 ± 45	54 ± 50	24 ± 26	NS
Ischemic cardiomyopathy	11	7	4	NS
Diabetes	11	7	4	NS
Hypertension	16	11	5	NS
Destination therapy	22	16	5	NS
Bridge to transplant	9	3	6	NS

Values are mean ± SD or n. *p Value between HMII and HVAD groups.
BSA = body surface area; HMII = HeartMate II; NS = not significant.

RV SHAPE ANALYSIS. The 3D RV endocardial surfaces were exported as a series of unstructured meshes of connected points that were used as input to custom software package for analysis of regional RV curvature (13). To accomplish this, a quadratic polynomial function was fit to the local neighborhood of each point belonging to the RV surface (bottom portion of **Figure 1**). This allowed computing, for each point, the values of curvature k_1 and k_2, each corresponding to the inverse of the radius of the 2 circles in orthogonal planes best fitting the local surface. The mean curvature, K, was then obtained by averaging the aforementioned 2 curvature values for each point. Finally, to compensate for changes in RV curvature secondary to changes in RV volume, the local value of the 3D curvature K was normalized (k_n) by the value of curvature of a sphere having the same instantaneous volume as the RV. Of note, zero curvature indicates a flat surface, whereas the more positive or negative values signify more convexity or concavity of the surface, respectively, from the perspective of a reference point outside the RV. Finally, the RV surface was divided into 2 distinct regions: septum and free wall. The regional 3D curvature K_n was obtained by averaging the values of all points within the region.

DATA AND STATISTICAL ANALYSIS. The numbers of patients that achieved successive stages of the ramp protocol are presented in **Table 2** for both the HMII and HVAD devices. Continuous variables were summarized as mean ± SD, whereas categorical variables were presented as absolute values and percentages. Comparisons were performed using the Student *t* test. Paired *t* tests were used when comparing results between different LVAD speeds. Categorical values were compared with the chi-square test. Statistical significance was defined as

FIGURE 1 Diagrammatic Representation of Computation of Shape Indices

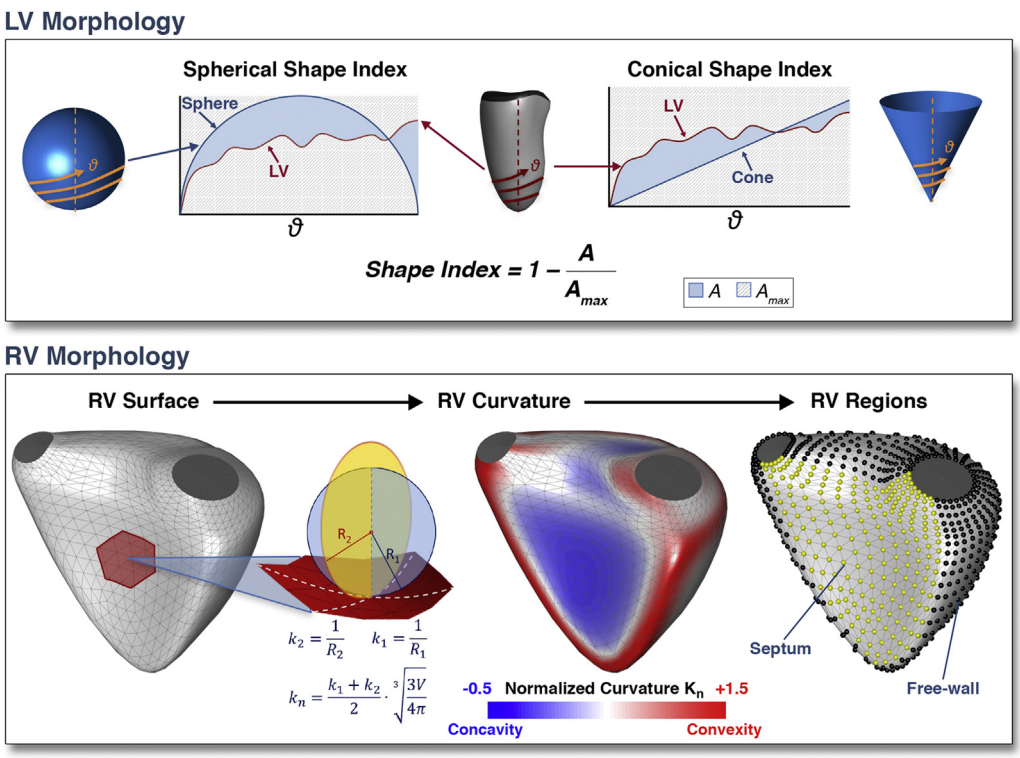

Computation of the sphericity and conicity indices of the left ventricle (LV) **(top)** and septal and free-wall curvature of the right ventricle (RV) **(bottom)** are shown. See text for details.

$p \leq 0.05$. To assess interobserver variability in volume and shape parameters, 15 RV and 15 LV datasets were remeasured by an independent observer who was blinded to the initial observer's results. This investigator also independently selected the best cardiac cycle for analysis. Interobserver variability was expressed in terms of percent variability, defined as the mean of the absolute differences between pairs of repeated measurements divided by their mean.

RESULTS

Baseline characteristics, as well as the breakdown between the HMII and HVAD subgroups, are presented in Table 1. The mean results of the 2D and 3D echocardiographic parameters for each stage are summarized in Table 3 for both cfLVADs. Patients were an average of 58 ± 11 years of age, and 35% had cfLVADs implanted for ischemic cardiomyopathy. Devices were used for destination therapy in 71% of patients. There were no significant differences between the HMII and HVAD groups in terms of age, sex distribution, ischemic etiology of cardiomyopathy, or reason for cfLVAD implantation.

Examples of 3D LV and RV endocardial surface reconstructions from a HMII patient and an HVAD patient are shown in Figures 2A and 2B, respectively; surfaces obtained at lowest RPM, shown by the gray frame for the LV and the red frame for the RV, and the highest RPM, shown by the orange frame for the LV and by the gray frame for the RV, are superimposed in each panel.

HeartMate II. From the cohort of 19 HMII patients, 97 3D LV datasets and 97 3D RV datasets were stored for analysis. Of the 97 LV images, 6 (6%) were of poor quality and not analyzable; of the 97 RV images collected, 8 (8%) were of poor image quality and not analyzable. Fifteen patients reached a maximum LVAD speed ≥10,800 RPM. Of the remaining 4 patients, 1 reached a maximum speed of 10,000 RPM, 2 reached a maximum speed of 10,400 RPM, and 1 reached a maximum speed of 9,600 RPM (Table 2, top).

Typical 3D images of the LV at the highest and lowest RPMs (superimposed) are shown in Figure 2A. Increasing pump speed resulted in decreases in chamber volume with a mean decrease in average volume of 127 ± 78 ml ($p < 0.01$) from lowest to highest speed setting (Figure 3A). In 16 of 19 (84%) patients, LV volumes decreased by ≥20% from the lowest to the highest speed setting. The progressive decrease in chamber volume was likely due to the LV walls moving toward the center, with some shortening of the base-to-apex dimension (mean base-to-apex dimension 9.6 ± 1.1 cm at the lowest RPM vs. 9.2 ± 1.1 cm at the highest RPM; $p = 0.001$); in tandem, the LV became more conical (less spherical) with increasing speeds (Figure 3B).

Averaged RV volumes did not change significantly until Stage IV of the protocol when volumes increased significantly (Figure 3A); this is also illustrated in the example of Figure 2A. On average, RV volume increased by ~60 ± 68 ml from the lowest to the highest stage ($p = 0.001$). Concomitantly, on average, the curvature of the interventricular septum increased (Figure 4, left panel), with the septum becoming more convex and bulging into the LV when comparing the lowest to the highest speed settings (0.97 ± 0.11 at lowest speed versus 1.03 ± 0.10 at highest speed; $p = 0.07$). Mean RV free-wall curvature decreased at higher speed as the RV free-wall became more concave (more flat) (1.22 ± 0.07 at lowest speed vs. 1.19 ± 0.04 at highest speed; $p = 0.07$). See Online Video 1.

HVAD. From the cohort of 12 HVAD patients, 56 3D full-volume LV and RV datasets were acquired. Of the 56 LV images, 2 (4%) were of poor quality and not analyzable; of the 56 RV images 5 (9%) were of poor image quality and not analyzable. Ten patients reached maximum speeds of ≥3,000 RPM; 2 were only able to reach a speed of 2,900 RPM. See the bottom of Table 2.

LV and RV endocardial surfaces from a representative HVAD patient are shown in Figure 2B. As seen in this example, there was little difference in global sphericity and conicity of the LV when comparing the lowest and highest speeds. Overall, with increasing speed, 3D LV volumes decreased by ~51 ± 38 ml ($p < 0.01$) (Figure 3C). This decrease was not as marked as was observed with HMII. With increasing speeds, the LV walls moved toward the center and a decrease in the base-to-apex dimension was seen. Mean base-to-apex dimension was 9.4 ± 1.4 cm at the lowest RPM versus 9.0 ± 1.4 cm at the highest RPM; $p = 0.09$. LV sphericity was higher for HVAD at the highest speed when compared with the HMII (0.71 ± 0.07 vs. 0.62 ± 0.07, respectively; $p = 0.004$) (Figure 3D). Interestingly, this difference between HVAD and HMII was not appreciated in the 2D LV dimension measurements made at the same speed (5.5 ± 1.1 cm vs. 5.1 ± 1.8 cm; $p = 0.50$) (Table 3). However, when linear LV dimensions at each stage were expressed as a fraction of the LV dimension at the lowest pump speed (% reduction in LV dimension), the linear dimension reductions were statistically significantly different between both devices (−13 ± 13% vs. 27 ± 16%; $p = 0.012$, for HVAD versus HMII, respectively) (Table 3). In contrast to the HMII, LV conicity and sphericity did not change significantly with increasing pump speeds in HVAD patients (Figure 3D).

The RV showed an overall trend to larger volumes with increasing cfLVAD speed by ~22 ± 42 ml ($p = 0.095$); the magnitude of this change was lower than was seen with HMII. Also in contrast to HMII patients, there were no changes in RV septal or free-wall curvature between the lowest and highest speed settings (0.94 ± 0.11 at lowest speed vs. 0.92 ± 0.18 at highest speed for mean septal curvature; $p = 0.57$; 1.22 ± 0.07 at lowest speed vs. 1.23 ± 0.06 at highest speed for mean free-wall curvature; $p = 0.43$). See Online Video 2.

TABLE 2 Number of Patients With Completed 3D Assessment at Successive Stages of the Ramp Protocol

RPM	Stage I	Stage II	Stage III	Stage IV	Stage V
HMII (n = 19)					
8,000	19				
8,400					
8,800		19			
9,200					
9,600			19		
10,000				18	
10,400				17	
10,800					15
11,200					11
11,600					4
HVAD (n = 12)*					
2,300	12				
2,400					
2,500		11			
2,600					
2,700			12		
2,800					
2,900				10	
3,000					10
3,100					8
3,200					5

*In the HVAD group, 1 patient did not have 3D assessment at Stage II.
3D = 3-dimensional; HMII = HeartMate II; RPM = revolutions per minute.

TABLE 3 Mean Echocardiographic Measurements for Each Stage of the Ramp Protocol

	Stage I	Stage II	Stage III	Stage IV	Stage V
HeartMate II					
Median pump speed, rpm	8,000	8,800	9,600	10,400	11,200
Flow, l/min	4 ± 1	5 ± 1	5 ± 1	6 ± 1	6 ± 1
PI	6 ± 1	6 ± 1	5 ± 1	4 ± 1	3 ± 1
Power, W	4 ± 1	5 ± 1	6 ± 1	7 ± 1	9 ± 1
CI, l/min/m^2	2 ± 1	2 ± 1	2 ± 1	3 ± 1	3 ± 2
RAP, mm Hg	12 ± 8	11 ± 7	11 ± 8	10 ± 7	11 ± 6
Systolic PAP, mm Hg	43 ± 11	41 ± 13	39 ± 13	36 ± 12	34 ± 10
Diastolic PAP, mm Hg	23 ± 8	21 ± 10	20 ± 9	18 ± 9	17 ± 9
Mean PAP, mm Hg	29 ± 9	28 ± 11	27 ± 10	24 ± 9	23 ± 9
PCWP, mm Hg	21 ± 10	17 ± 8	14 ± 8	11 ± 6	11 ± 5
PA saturation, %	56 ± 9	59 ± 9	62 ± 8	65 ± 7	68 ± 7
BP, Doppler, mm Hg	87 ± 20	91 ± 18	96 ± 17	100 ± 19	99 ± 19
LV EDD, cm	6.6 ± 1.4	6.2 ± 1.5	6.0 ± 1.5	5.6 ± 1.7	5.1 ± 1.8
% Reduction in LV EDD*	0 ± 0	−8 ± 6	−11 ± 8	−14 ± 10	−27 ± 16
% With AV opening†	53	37	22	12	7
LV EDV, ml	320 ± 133	302 ± 139	263 ± 138	253 ± 129	184 ± 129
LV conicity	0.73 ± 0.03	0.74 ± 0.04	0.76 ± 0.04	0.77 ± 0.03	0.79 ± 0.04
LV sphericity	0.72 ± 0.07	0.71 ± 0.07	0.67 ± 0.06	0.66 ± 0.05	0.62 ± 0.07
RV EDV, ml	248 ± 116	281 ± 124	277 ± 124	325 ± 118	349 ± 147
RV septal curvature	0.97 ± 0.11	1.00 ± 0.11	1.03 ± 0.13	0.98 ± 0.14	1.02 ± 0.11
RV free-wall curvature	1.22 ± 0.07	1.20 ± 0.06	1.19 ± 0.05	1.20 ± 0.06	1.19 ± 0.04
HVAD					
Median pump speed, rpm	2,300	2,500	2700	2,900	3,150
Flow, l/min	3 ± 1	4 ± 1	4 ± 1	4 ± 1	5 ± 1
PI	4 ± 1	4 ± 1	3 ± 1	3 ± 1	3 ± 1
Power, W	2 ± 0	3 ± 0	4 ± 0	5 ± 0	6 ± 1
CI, l/min/m^2	2 ± 1	2 ± 0	2 ± 0	2 ± 0	3 ± 1
RAP, mm Hg	9 ± 7	10 ± 7	9 ± 7	9 ± 8	10 ± 8
Systolic PAP, mm Hg	45 ± 16	44 ± 15	42 ± 12	41 ± 14	43 ± 11
Diastolic PAP, mm Hg	24 ± 10	23 ± 10	23 ± 9	21 ± 10	21 ± 7
Mean PAP, mm Hg	31 ± 12	30 ± 11	29 ± 10	27 ± 11	29 ± 9
PCWP, mm Hg	18 ± 7	17 ± 7	15 ± 7	13 ± 8	13 ± 7
PA saturation, %	59 ± 7	60 ± 6	61 ± 5	64 ± 4	67 ± 4
BP, Doppler, mm Hg	89 ± 7	88 ± 8	89 ± 8	89 ± 11	88 ± 7
LV EDD, cm	6.3 ± 0.6	6.1 ± 0.7	6.0 ± 0.8	5.7 ± 0.9	5.5 ± 1.1
% Reduction in LV EDD*	0 ± 0	−2 ± 3	−5 ± 6	−8 ± 3	−13 ± 13
% With AV opening†	91	82	42	18	10
LV EDV, ml	301 ± 77	276 ± 76	280 ± 76	271 ± 72	248 ± 93
LV conicity	0.73 ± 0.03	0.73 ± 0.03	0.74 ± 0.02	0.73 ± 0.02	0.74 ± 0.04
LV sphericity	0.72 ± 0.05	0.73 ± 0.05	0.72 ± 0.05	0.73 ± 0.04	0.71 ± 0.07
RV EDV, ml	238 ± 123	230 ± 90	254 ± 92	258 ± 127	279 ± 107
RV septal curvature	0.94 ± 0.11	0.81 ± 0.36	0.91 ± 0.13	0.86 ± 0.18	0.98 ± 0.09
RV free-wall curvature	1.21 ± 0.08	1.24 ± 0.08	1.24 ± 0.06	1.24 ± 0.07	1.24 ± 0.05

Values are mean ± SD. *% Reduction in LV EDD is determined by calculating the ratio in % between measured LV EDD at a given stage and LV EDD at the lowest pump speed. For example, for Stage II: % reduction in LV EDD = (LV EDD$_{(Stage\ II)}$ − LV EDD$_{(Stage\ I)}$)/LV EDD$_{(Stage\ I)}$ × 100%. †Refers to the % of patients with aortic valve opening (intermittent or every beat) at that stage.

AV = aortic valve; BP = blood pressure; CI = cardiac index; EDD = end-diastolic diameter; EDV = end-diastolic volume; HMII = HeartMate II; LV = left ventricular; PA = pulmonary artery; PAP = pulmonary artery pressure; PCWP = pulmonary capillary wedge pressure; PI = pulsatility index; RAP = right atrial pressure; RV = right ventricular.

INTEROBSERVER VARIABILITY. Interobserver variability for volume and shape parameters as reflected by percent variability was 15% for LV volume, 11% for RV volume, 7% for LV sphericity, 9% for RV free-wall curvature, and 7% for RV septal curvature.

DISCUSSION

The incidence of heart failure is increasing at an alarming rate, with more than 700,000 new cases being diagnosed each year in the United States (2,14).

Approximately one-half of these cases have heart failure with reduced ejection fraction, with many failing medical management, requiring mechanical circulatory support either as bridge to transplant or destination therapy. In the United States, the Food and Drug Administration has approved only 2 circulatory support devices: the HMII and the HVAD. The majority of cfLVADs today are being implanted as destination therapy (2,15). Seventy percent of patients supported with cfLVAD will live more than 2 years, whereas 50% will live more than 4 years (2). Maintenance of quality of life in patients with LVADs is therefore of high importance, including the optimization of cfLVAD speed settings.

This is the first study to our knowledge to report the LV and RV shape changes in response to speed in patients supported with either HMII or HVAD. Our main findings were as follows: in patients supported with HMII pumps, LV volumes decrease, the LV cavity becomes more conical, and less spherical, with advancing pump speeds and augmented LV unloading. On average, in patients who were able to tolerate speeds beyond 9,600 RPM, RV volumes tended to increase, with the RV septum bulging into the LV at the highest speeds. By contrast, in patients supported with the HVAD, the LV showed a more modest reduction in volume with no significant changes in conicity and sphericity. Additionally, there was less increase in RV volume with no change in the septum location in these patients at higher speeds.

In contrast to the differential volume and shape responses during ramp studies between these 2 pumps, we recently reported that both HVAD and HMII pumps displayed similar short-term hemodynamic responses (in terms of changes in pulmonary capillary wedge pressure, central venous pressure, and total cardiac output) at advancing stages (6). The differential responses between echocardiographic-based volume and shape parameters and hemodynamic findings in HVAD and HMII patients may have an implication on patient selection for each of these devices.

DIFFERENTIAL BEHAVIOR BETWEEN HVAD AND HMII PUMPS. Both HMII and HVAD pumps are continuous flow devices. The HMII pump is an axial flow device in which blood outflow is directed parallel to the axis of rotor or impeller rotation; it is situated in the subdiaphragmatic pocket. The HVAD pump is a centrifugal device situated in the thorax wherein impeller and therefore blood flow is directed perpendicular to the axis of rotation (**Figure 5**) (4). Previous studies based on 2D echocardiographic measurements have shown that HVADs result in less of a reduction in LV chamber diameter with increasing speed compared with HMII pumps (16,17). Recently, we reported that these pumps provide similar overall flows in the normal working range of speed (6), therefore, a possible explanation for the differential shape changes seen in this study during unloading is the location of the pumps in the body. The HMII pump is located subdiaphragmatically, likely resulting in inferior displacement of the LV apex due to the pull of the inflow cannula. By contrast, the HVAD pump is inserted intrathoracically at the LV apex, resulting in less distortion of the LV apex (6) (**Figure 5**). In this way, it is possible that the HVAD pump causes less deformation at the base of the heart due to the limited space in the chest.

RV CHANGES AT HIGHER LVAD SPEEDS. The use of 2D echocardiography to optimize LVAD speed settings is a relatively recent practice, and the impact of echocardiography-guided LVAD speed adjustment on outcomes is unknown (3,6,14,15). The ability to measure RV and LV volumes and endocardial shape during incremental ramp test stages enables appreciation

FIGURE 2 3D Endocardial Surfaces of the LV and RV in Representative Patients With a HMII and a HVAD Device

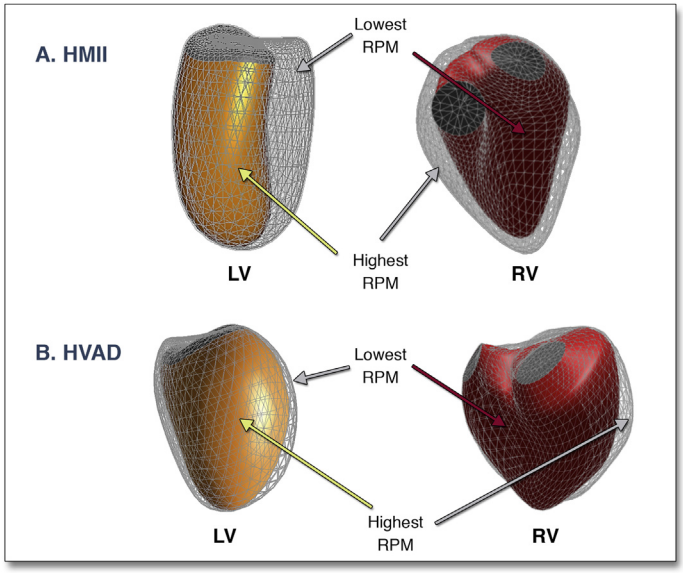

The 3-dimensional (3D) endocardial surfaces of the LV **(orange)** and RV **(red)** were obtained at the lowest and highest revolutions per minute (RPM) in a representative patient with a HeartMate II (HMII) device **(A)** and with a HVAD device **(B)**. Surfaces obtained at lowest RPM, shown by the **gray frame** for the LV and the **red frame** for the RV and the highest RPM, shown by the **orange frame** for the LV and by the **gray frame** for the RV are superimposed in each panel. See text for details. RPM = revolutions per minute; other abbreviations as in **Figure 1**. See Online Videos 1 and 2.

FIGURE 3 Effect of Increasing Speed on LV and RV Volumes and LV Shape

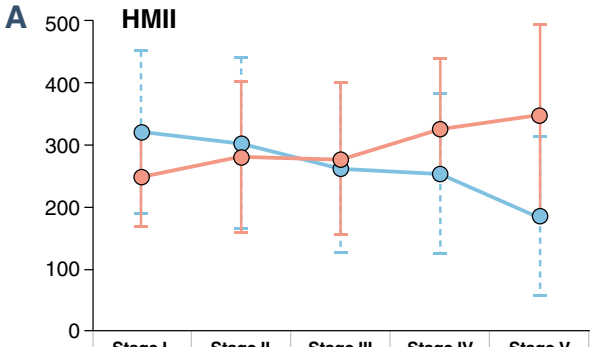

	Stage I 8000 RPM	Stage II 8800 RPM	Stage III 9600 RPM	Stage IV 10400 RPM	Stage V 11200 RPM
LV Volume	320.20	302.21	262.64	253.21	184.44
RV Volume	248.18	280.54	276.92	325.06	348.99

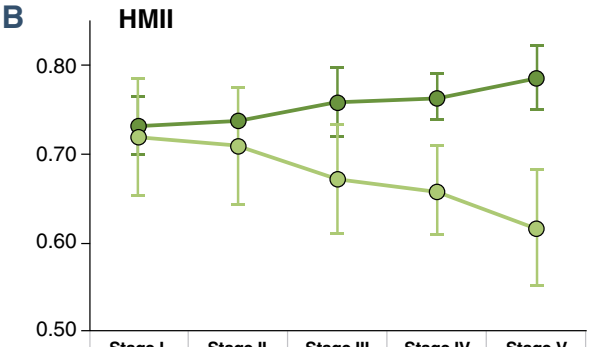

	Stage I 8000 RPM	Stage II 8800 RPM	Stage III 9600 RPM	Stage IV 10400 RPM	Stage V 11200 RPM
LV Conicity	0.73	0.74	0.76	0.77	0.79
LV Sphericity	0.72	0.71	0.67	0.66	0.62

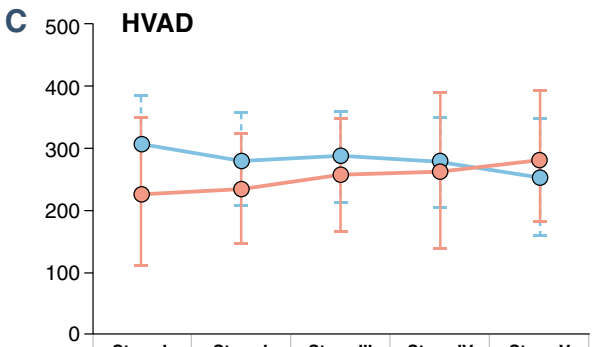

	Stage I 2300 RPM	Stage I 2500 RPM	Stage III 2700 RPM	Stage IV 2900 RPM	Stage V 3150 RPM
LV Volume	300.68	276.05	280.21	271.17	248.29
RV Volume	223.41	229.65	253.53	257.70	279.47

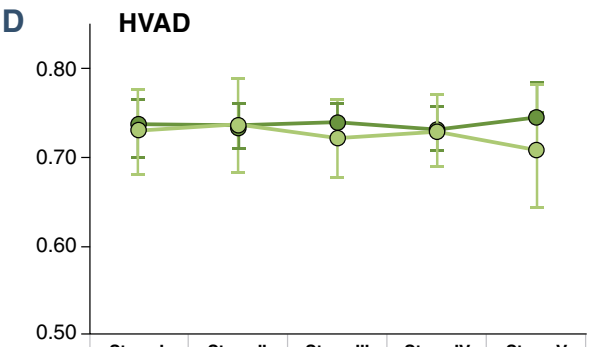

	Stage I 2300 RPM	Stage II 2500 RPM	Stage III 2700 RPM	Stage IV 2900 RPM	Stage V 3150 RPM
LV Conicity	0.73	0.73	0.74	0.73	0.74
LV Sphericity	0.72	0.73	0.72	0.73	0.71

In the HMII cohort **(top)**, 3D LV volumes decreased progressively as speed increased **(A, blue line)** and the LV cavity became progressively less spherical and more conical **(B)**. Averaged RV volumes did not change significantly until Stage IV, at which point, volumes increased significantly **(A, red line)**. In the HVAD cohort, similar, although more subtle changes were seen in LV and RV volumes with increasing speeds (**A, blue line,** LV; **and red line,** RV). No difference was seen in LV conicity or sphericity with increasing speed. Abbreviations as in Figures 1 and 2.

for the counteracting effects of LVAD speed on the RV. On one hand, increased speed leads to decreased pulmonary capillary wedge pressure, thereby reducing the afterload on the RV and facilitating RV function. On the other hand, increasing speeds result in increased venous return to the RV and septal shift toward the LV, which increases RV preload and potentially decreases RV contractility due to the abnormal geometry. At low-to-moderate speeds, these effects counterbalance each other, so there is no net effect on RV size and function. At higher LVAD speeds, the septal shift and increased venous return appear to dominate. The pump speed at which the balance tips can be identified if RV size parameters are systematically measured throughout the ramp study to determine the "cross-over point" between LV decompression and RV enlargement. One possible concern is that setting a pump speed higher than this cross-over point could result in clinically relevant RV failure, which could manifest over time However, further studies are warranted to better understand this possibility.

In keeping with the "cross-over" point, it is noteworthy that, at least in HMII pumps, RV septal curvature changes from the lowest to highest speed, suggesting that a calculated measure of septal curvature from 2D images could also be used to choose a more physiological LVAD speed. Interestingly, not all patients showed an increase in curvature from lowest to highest speed settings. Some of this

FIGURE 4 Effect of Increasing Speed on the Right Ventricle Free-Wall and Septum

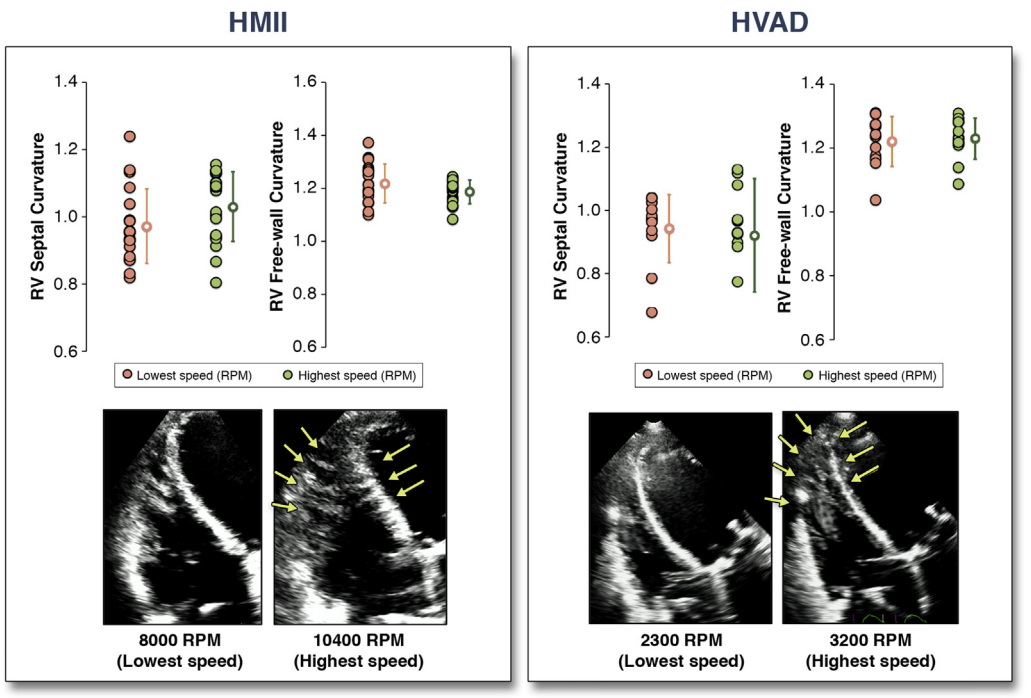

In the HMII cohort, on average, the interventricular septum **(top, far left)**, became more convex, bulging into the LV when comparing the lowest to the highest speed settings. This is illustrated on 2D echocardiography in a representative patient, bottom left. The **yellow arrows** illustrate septal bulging. Meanwhile, the RV free-wall became flatter at increased speeds. In the HVAD cohort, on average, the curvature of the interventricular septum did not change significantly when comparing the lowest to the highest speed settings (**top, right,** and 2-dimensional image in a representative patient, **bottom right**). Mean RV free-wall curvature did not change when comparing lowest to highest speed setting **(top, far right).** Abbreviations as in Figures 1 and 2.

FIGURE 5 Representative Chest X-Rays Illustrating the Location of the HMII and the HVAD in the Thoracoabdominal Cavity

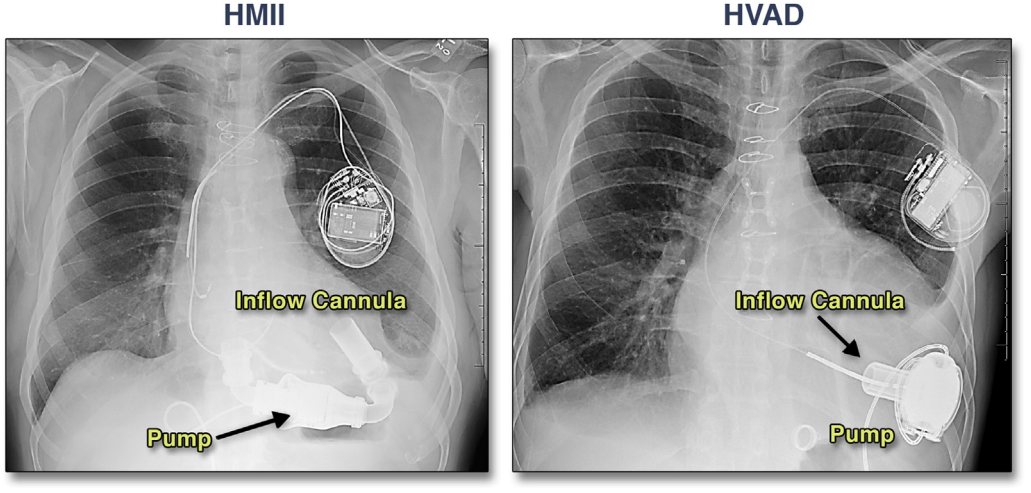

The HMII is located subdiaphragmatically **(left)**, whereas the HVAD pump is inserted intrathoracically at the LV apex **(right)**. Abbreviations as in Figures 1 and 2.

variability may be due to inflow cannula orientation, which differs significantly between patients. Alternatively, the variability in septal shifts could be determined by net LV volume reduction and RV overload regardless of the inflow cannula orientation. Further study is required to better understand this finding.

As a final point, in our study, 3D echocardiography was feasible in only 56% of patients, in part due to the difficulties associated with patient positioning. Most patients had to be scanned in the supine position because simultaneous right heart catheterization was being performed. We only included patients with adequate LV and RV 3D imaging. If only 1 chamber could be imaged, the patient was not included because we were interested in the paired response of the LV and RV. Additionally, 3D imaging was challenging in obese patients, in those with poor 2D image quality, and in those with very large ventricles, which were difficult to fit in the 3D sector. Some of these had to be excluded. In the non-LVAD population, feasibility for 3D LV dataset acquisition is in the 85% range. However, feasibility of 3D RV acquisition is lower. Given these difficulties, development of a 2D ramp protocol including apical RV-focused views to assess RV septal curvature, as well as the "cross-over point" by measurement of RV end-diastolic dimensions and area, as well as degree of tricuspid regurgitation, may constitute a future alternative.

STUDY LIMITATIONS. This is a single-center study consisting of pooled data of a relatively small number of patients. Additionally, 3D echocardiography was only feasible in 56% of patients undergoing LVAD ramp studies. The interpatient variability of RV septal and free-wall curvature could have been better accounted for if concomitant knowledge of inflow cannula position was available. This was not possible using the data collected in this study. Finally, we only considered changes in LV and RV geometry in response to short-term changes in cfLVAD speed. Long-term geometric responses to such changes could be different, and the long-term clinical consequences of observed changes in terms of mortality, improved morbidity, greater or lower likelihood of RV failure or recovery remain unknown.

CONCLUSIONS

Although the use of 3D echocardiography for patients undergoing echocardiography-guided ramp studies for cfLVAD speed optimization is technically challenging and time consuming, the current study provides valuable insight on the impact of different cfLVAD speed settings on the volumes and shapes of both ventricles. We have shown that with careful assessment, it is possible to determine a "cross-over point" in HMII patients at which speed there is excessive LV decompression, which may be coupled with undesirable RV dilatation. Our study suggests that HMII and HVAD pumps have different impacts on RV and LV volumes and shape, which may be due to the different anatomic positions in the thoracoabdominal cavity. Future studies on quality of life and outcomes using this information may provide additional insight into the optimal speed choice for the destination cfLVAD.

ADDRESS FOR CORRESPONDENCE: Dr. Roberto M. Lang, University of Chicago Medicine, 5758 S. Maryland Avenue, MC 9067, DCAM 5509, Chicago, Illinois 60637. E-mail: rlang@medicine.bsd.uchicago.edu.

PERSPECTIVES

COMPETENCY IN MEDICAL KNOWLEDGE: Optimization of LVAD function is important for patient quality of life. By combining hemodynamic data with 3D echocardiographic indices of LV and RV volume and shape, we were able to show that while the LV decreases in volume and becomes more conical with increasing pump speeds, the RV, in contrast, increases in size at higher speeds. This finding may impact patients at higher speed settings. Further to this observation, we were also able to demonstrate that increasing pump speeds had a differential impact on the Heart Mate II pumps and the HVAD pumps (the 2 most widely available pumps on the market). Higher pump speeds showed greater impact on LV and RV morphology in patients with the HeartMate II pump that in those with a HVAD.

TRANSLATIONAL OUTLOOK: Insight into LV and RV shape and morphology with increasing pump speeds may have an impact on LVAD speed optimization. Future studies should investigate whether speeds chosen to avoid RV enlargement and optimize LV shape would alter patient outcomes in terms of morbidity and/or mortality, and whether the differential impact on LV and RV morphology between the HVAD and HeartMate II is clinically significant in terms of outcomes.

REFERENCES

1. Feldman D, Pamboukian SV, Teuteberg JJ, et al. The 2013 International Society for Heart and Lung Transplantation guidelines for mechanical circulatory support: executive summary. J Heart Lung Transplant 2013;32:157–87.

2. Kirklin JK, Naftel DC, Pagani FD, et al. Seventh INTERMACS annual report: 15,000 patients and counting. J Heart Lung Transplant 2015;34:1495–504.

3. Uriel N, Morrison KA, Garan AR, et al. Development of a novel echocardiography ramp test for speed optimization and diagnosis of device thrombosis in continuous-flow left ventricular assist devices: the Columbia ramp study. J Am Coll Cardiol 2012;60:1764–75.

4. Uriel N, Levin AP, Sayer GT, et al. Left ventricular decompression during speed optimization ramps in patients supported by continuous-flow left ventricular assist devices: device-specific performance characteristics and impact on diagnostic algorithms. J Card Fail 2015;21:785–91.

5. Moazami N, Fukamachi K, Kobayashi M, et al. Axial and centrifugal continuous-flow rotary pumps: a translation from pump mechanics to clinical practice. J Heart Lung Transplant 2013;32:1–11.

6. Uriel N, Sayer G, Addetia K, et al. Hemodynamic ramp tests in patients with left ventricular assist devices. J Am Coll Cardiol HF 2016;4:208–17.

7. Drakos SG, Janicki L, Horne BD, et al. Risk factors predictive of right ventricular failure after left ventricular assist device implantation. Am J Cardiol 2010;105:1030–5.

8. Kormos RL, Teuteberg JJ, Pagani FD, et al. Right ventricular failure in patients with the HeartMate II continuous-flow left ventricular assist device: incidence, risk factors, and effect on outcomes. J Thorac Cardiovasc Surg 2010;139:1316–24.

9. Topilsky Y, Hasin T, Oh JK, et al. Echocardiographic variables after left ventricular assist device implantation associated with adverse outcome. Circ Cardiovasc Imaging 2011;4:648–61.

10. Lang RM, Badano LP, Tsang W, et al. EAE/ASE recommendations for image acquisition and display using three-dimensional echocardiography. J Am Soc Echocardiogr 2012;25:3–46.

11. Maffessanti F, Lang RM, Corsi C, Mor-Avi V, Caiani EG. Feasibility of left ventricular shape analysis from transthoracic real-time 3-D echocardiographic images. Ultrasound Med Biol 2009;35:1953–62.

12. Maffessanti F, Caiani EG, Tamborini G, et al. Serial changes in left ventricular shape following early mitral valve repair. Am J Cardiol 2010;106:836–42.

13. Addetia K, Maffessanti F, Yamat M, et al. Three-dimensional echocardiography-based analysis of right ventricular shape in pulmonary arterial hypertension. Eur Heart J Cardiovasc Imaging 2016;17:564–75.

14. Stainback RF, Estep JD, Agler DA, et al. Echocardiography in the management of patients with left ventricular assist devices: recommendations from the American Society of Echocardiography. J Am Soc Echocardiogr 2015;28:853–909.

15. Mancini D, Colombo PC. Left ventricular assist devices: a rapidly evolving alternative to transplant. J Am Coll Cardiol 2015;65:2542–55.

16. Lalonde SD, Alba AC, Rigobon A, et al. Clinical differences between continuous flow ventricular assist devices: a comparison between HeartMate II and HeartWare HVAD. J Card Surg 2013;28:604–10.

17. Sauer AJ, Meehan K, Gordon R, et al. Echocardiographic markers of left ventricular unloading using a centrifugal-flow rotary pump. J Heart Lung Transplant 2014;33:449–50.

KEY WORDS 3-dimensional echocardiography, conicity, continuous-flow LVAD, curvature, ramp study, sphericity, ventricular shape

APPENDIX For supplemental videos and their legends, please see the online version of this paper.